ERNEST ORLANDO LAWRENCE
BERKELEY NATIONAL LABORATORY

Energy Performance Assessment of Ventilation Systems in Korean Apartments with Radiant Floor Heating: Final Report

Craig Wray, Max Sherman
Environmental Energy Technologies Division
Lawrence Berkeley National Laboratory
USA

Damien Gondre
Département Génie Energétique et Environnement
Institut National des Sciences Appliquées de Lyon
France

Yun-Gyu Lee
Building Planning and Environment Research Division
Korea Institute of Construction Technology
Korea

April 2011

This work was supported by the Assistant Secretary for Energy Efficiency and Renewable Energy, Office of Building Technology, State, and Community Programs, of the U.S. Department of Energy under Contract No. DE-AC02-05CH11231, and by GREX Electronics Co., Ltd. under Work for Others Agreement No. WF006874.

INTRODUCTION

Traditional Korean houses relied on leaky construction and infiltration/natural ventilation driven by stack and wind pressures to remove pollutants and provide acceptable indoor air quality. As new buildings shifted from houses to apartment buildings and buildings became more airtight, there were concerns about poor indoor air quality and associated health complaints. Beginning in 2006, the Korean government imposed a ventilation standard that requires using mechanical ventilation in new and remodeled apartment buildings to provide a minimum ventilation rate of 0.7 air changes per hour (ACH).

Floor panels supplied with hot water from a hydronic system are commonly used to radiantly heat apartments. Heat recovery ventilators (HRVs) are the primary means of providing mechanical ventilation. An HRV uses fans and duct networks to supply outdoor air to and exhaust indoor air from conditioned spaces. It includes an internal heat exchanger to transfer sensible heat from the exhaust air to the supply air, and an electrically-powered preheater that operates when needed to warm cold supply air to an acceptable temperature before entering the HRV (for frost control) and then conditioned spaces (comfort control).

To eliminate electric preheating, GREX has invented a system that uses a fan to supply ventilation air through ducts embedded in lightweight concrete between floor radiant heating panels and an insulation layer beneath the panels. Heat transfer from the floor preheats the supply air before it enters the conditioned spaces. In one version of the system, air leaves the conditioned space by exfiltration through envelope and inter-apartment leaks, as well as through intermittently-open windows. To prevent excessive pressurization of the conditioned spaces, an exhaust system consisting of bathroom exhaust fans and ducts located in ceiling plenums is used. To assess the annual energy performance of the non-HRV (hereafter referred to as GREX) system relative to the conventional HRV system, Lawrence Berkeley National Laboratory (LBNL) developed and carried out coupled iterative minute-by-minute computer simulations of a hypothetical multizone apartment building with floor radiant heating. The remainder of this report summarizes our simulation approach, the inputs used in the simulations, and the simulation results.

SIMULATION APPROACH

Our initial simulation approach was to create a geometric model of a hypothetical twenty-floor apartment building using a Google SketchUp plugin for TRNSYS and building characteristics provided by GREX, and then to simulate the energy performance of each system using the model, TRNSYS, and CONTAM. TRNSYS is a modular program that can simulate the thermal performance of building components and HVAC systems, assuming that airflows throughout the system are known. CONTAM is a separate modular program that can simulate airflows, pressures, and contaminant transport in multizone compartmented buildings, assuming that temperatures throughout the airflow network are known. More specifically, our plan was to assign thermal nodes to each space within the building, to use TRNSYS to calculate air and surface temperatures at each thermal node, and to use CONTAM to calculate airflows and pressures between spaces and across the building envelope.

We chose this approach because TRNSYS and CONTAM apparently had been used together in the past to study combined heat transfer and ventilation in multi-storey office buildings (McDowell et al. 2003). As a result, links to support information transfer between the thermal and airflow analyses at each iteration step are already available within TRNSYS. However, upon further review, we found that that CONTAM itself is not directly coupled with TRNSYS.

Instead, CONTAM can be used to generate an input file that TRNSYS then reads and uses in an internal calculation module (Type 97) that is loosely based on a precursor to CONTAM (AIRNET). AIRNET and the internal module in TRNSYS also can simulate airflows and pressures (but not contaminant transport) in multizone compartmented buildings. The internal module, however, has very limited input capabilities compared to AIRNET and CONTAM, which meant that some features such as pressure-dependent fan and duct airflows could not be simulated.

We also found that links between the TRNSYS building module (Type 56) and its airflow calculation module (Type 97) must be manually configured. For a twenty-storey building with four apartments per floor, four internal zones per apartment, enclosed balconies on two sides of each apartment, and multiple leaks between each zone, thousands of these links needed to be configured, which is impractical. As a result, we reduced the scope of our simulations to a single apartment with two internal zones and balconies on the north and south faces.

Furthermore, during model development of the four zone configuration, we found that with constant outdoor temperature and constant wind, infiltration and exfiltration airflows and related pressures calculated using CONTAM and then using the TRNSYS internal airflow/pressure solver did not match. In particular, there were substantial differences between the infiltration and exfiltration airflows calculated using the two methods, and large imbalances in infiltration and exfiltration flows in the internal module, especially for windy conditions. The source of these errors is unknown. To overcome this envelope leakage simulation problem, we did not use the internal airflow calculation module (Type 97). Instead, we created a new calculation module in TRNSYS to implement the LBNL single zone "infiltration" model (ASHRAE 2009a) and linked it to the TRNSYS building module. This approach is suboptimal, but provides a crude means of estimating infiltration and exfiltration airflows that is consistent with the airflow network as a whole: (1) all mechanical system flows are balanced and constant, which means that they have no effect on building pressures and therefore on infiltration and exfiltration, and (2) principal airflows occur through mechanical systems and intermittently open windows and doors.

SIMULATION INPUT DATA

Weather

South Korea is located in East Asia, on the southern half of the Korean Peninsula. It experiences a large temperature difference between summer and winter with a cold and dry winter and a hot and humid summer (Lee and Kim 2008). The country is often divided into three climates zones represented by large cities (Lee and Kim 2008): north (Seoul, 10.4 million people), central (Daegu, 2.5 million people), and south (Busan, 3.6 million people). In the northern region, which is affected by the continental climate, a building must be able to withstand the colder climate. The southern region is affected more by the subtropical climate and is pleasant most of the year. However, the summers in this region are humid, so ventilation and lightweight structures are essential to avoid overheating. The climate in the central region falls between the climates of the northern and the southern regions (Yeo et al. 2003).

We initially acquired weather data files for each climate region (Seoul, Busan, and Daegu). These files include hourly dry-bulb temperature, humidity ratio, beam solar radiation, wind direction, and wind speed for one year. Unfortunately, these files included what appear to be cloud cover fractions and not the appropriate diffuse solar radiation data required for use in TRNSYS. As a result, we used the TRNSYS-supplied hourly MeteoNorm TMY2-format weather file for Seoul instead. TRNSYS files for Busan and Daegu currently are not available.

Apartment Geometry and Ventilation System Configurations

Figure 1 and Figure 2 show the apartment geometry and two ventilation system configurations, with supply air ducts in blue (Figure 1) or green (Figure 2) and exhaust air ducts in red. North is assumed to be at the top of the drawings.

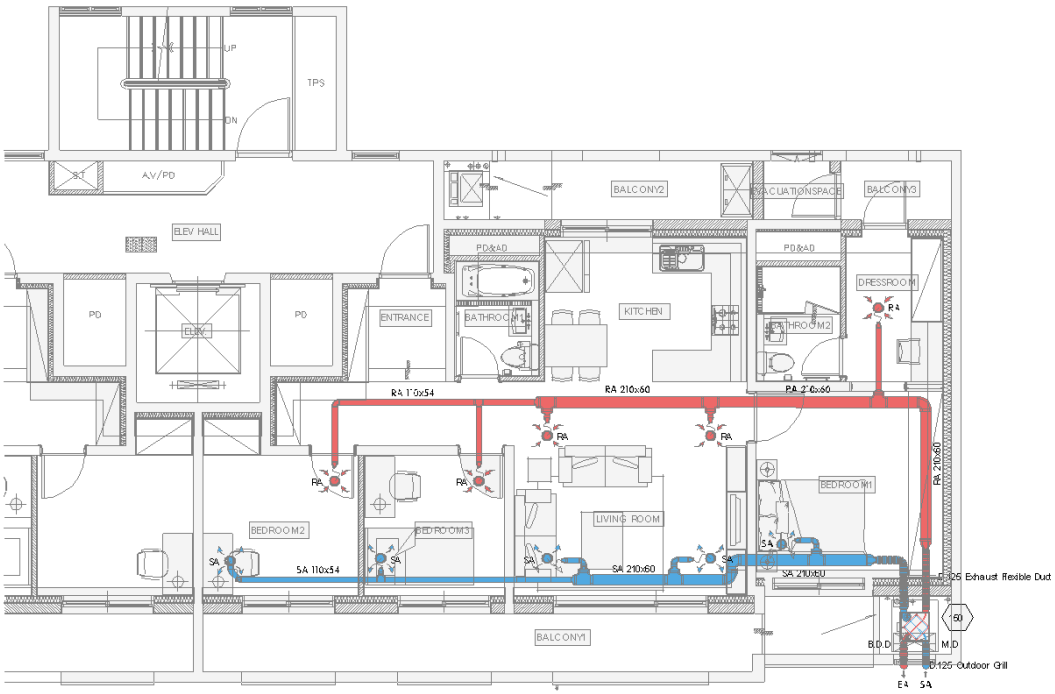

Figure 1: HRV system

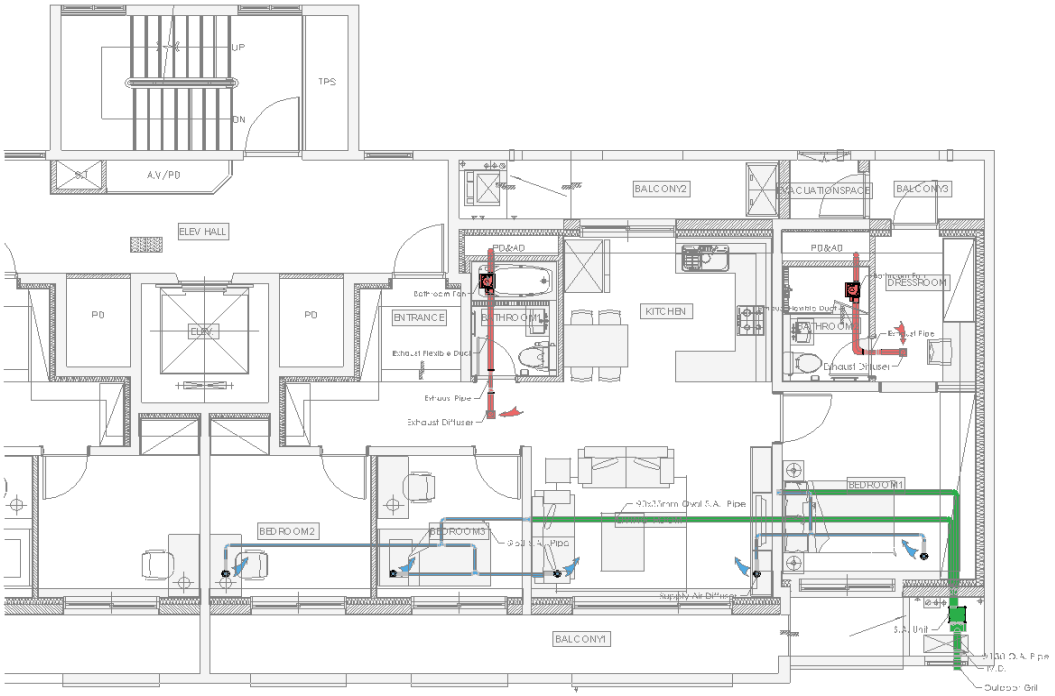

Figure 2: GREX system (non-HRV)

To clarify the geometry in Figure 1 and Figure 2, we assigned a name and a number to each room within the apartment and the related service shafts as shown in Figure 3 and Table 1.

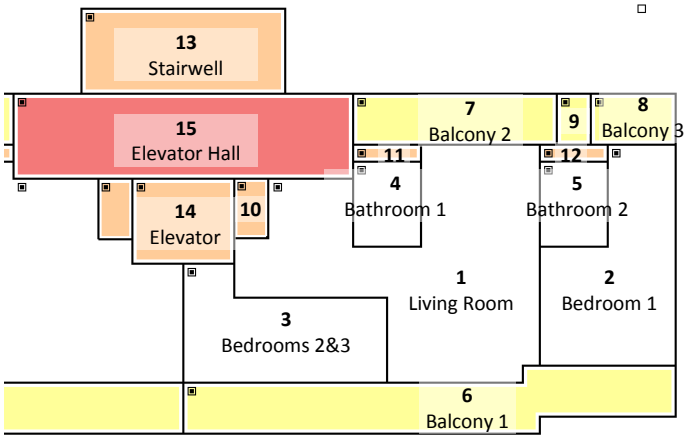

Figure 3: Room configuration

	Space
1	Living Room (with kitchen)
2	Bedroom 1
3	Bedroom 2&3
4	Bathroom 1
5	Bathroom 2
6	Balcony 1
7	Balcony 2
8	Balcony 3
9	Evacuation Space
10	Plumbing duct 2
11	Plumbing duct 3
12	Plumbing duct 4
13	Stairwell
14	Elevator
15	Elevator Hall

Table 1: Space list

As described in the Simulation Approach section, to simplify the modeling, we divided the apartment into four thermal zones. One interior zone (A) includes bedrooms 2 and 3, the living room (with kitchen), and bathroom 1. A second interior zone (B) includes bedroom 1 and bathroom 2. The North balcony zone includes balconies 2 and 3 and the evacuation space between them. The South balcony includes balcony 1. Stairwells, elevator shafts, and plumbing ducts (PD) are not included. Figure 4 through Figure 6 show the four zone layout.

Table 2 lists the component surface areas and glazing fractions. Interior zone thermal capacitances account for furnishings and are based on California Title 24 (CEC 2008) approximations: 71.6 kJ/(m^2 K). Balcony zone thermal capacitances are based on multiplying zone volume, standard air density (1.2 kg/m^3), and a factor of 5 as suggested by TRNSYS staff.

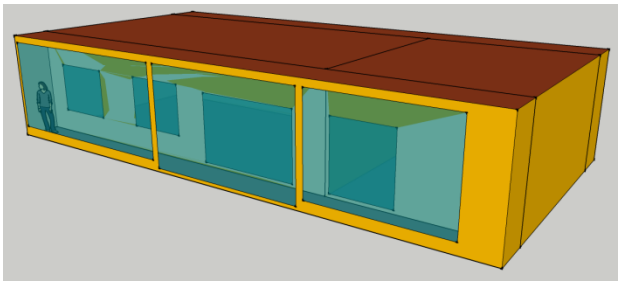

Figure 4: Southeast exterior view of apartment model

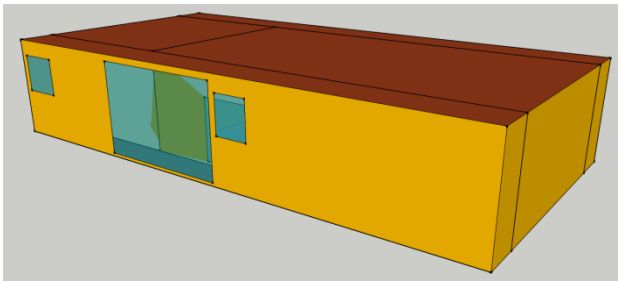

Figure 5: Northwest exterior view of apartment model

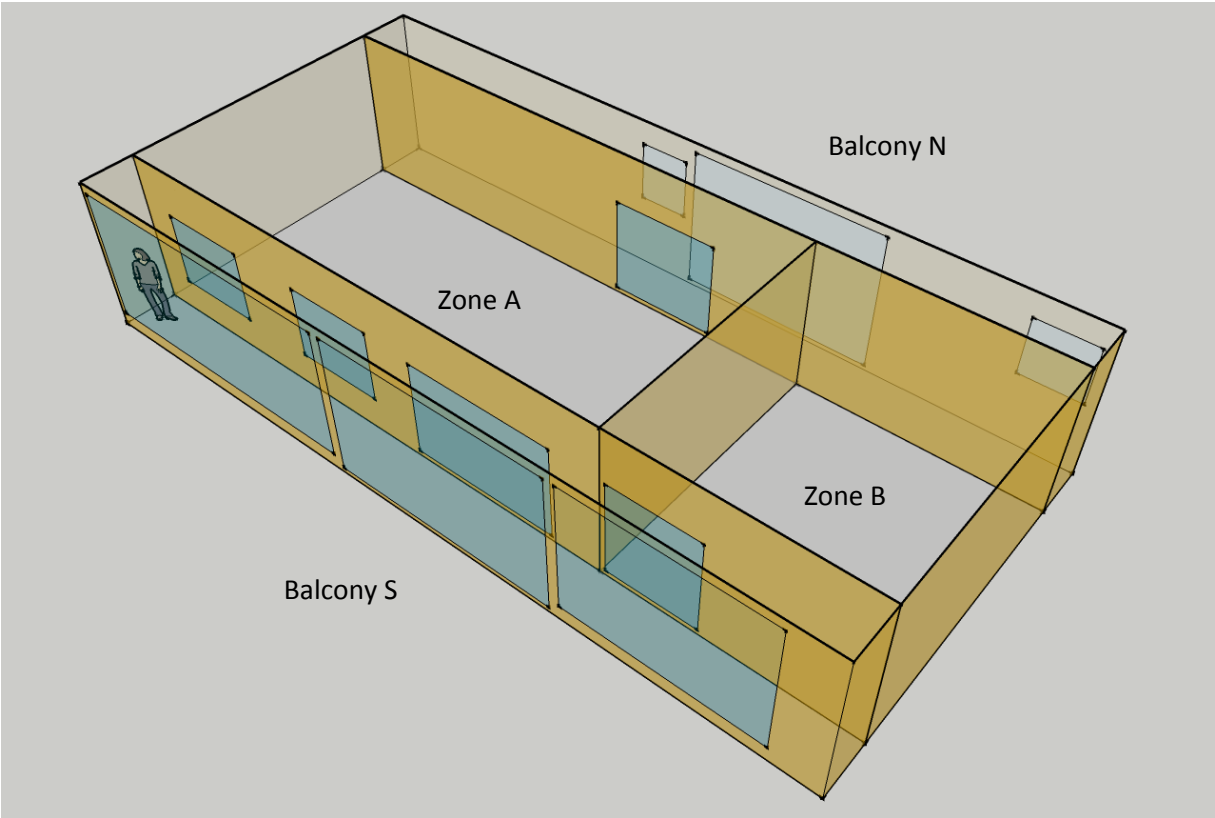

Figure 6: Apartment model layout – Sectional view

Zone	Volume (m^3)	Thermal Capacitance (kJ/K)	Component	Opaque Area (m^2)	Glass Area (m^2)	Total Area (m^2)	Glass Fraction (%)
Interior A	192.85	4311	Floor/ceiling (each)	60.3	0	60.3	0
			S wall	23.2	11.4	34.6	33.0
			N wall	30.2	4.4	34.6	12.7
			E/W wall (each)	17.9	0	17.9	0
Interior B	86.42	1932	Floor/ceiling (each)	27.0	0	27.0	0
			S wall	11.9	3.6	15.5	23.2
			N wall	15.5	0	15.5	0
			E/W wall (each)	17.9	0	17.9	0
Balcony S	55.05	330	Floor/ceiling (each)	17.2	0	17.2	0
			S wall	10.8	39.3	50.1	78.4
			E/W wall (each)	3.5	0	3.5	0
Balcony N	55.05	330	Floor/ceiling (each)	17.2	0	17.2	0
			N wall	35.9	14.2	50.1	28.5
			E/W wall (each)	3.5	0	3.5	0

Table 2: Apartment component surface areas

Material Properties

Table 3 lists the material properties for opaque elements in the building model. Insulation thicknesses are based on Kim et al. (2009). Convection coefficients for surfaces are based on TRNSYS defaults for interior and exterior surfaces: 3.1 W/(m^2 K) and 18 W/(m^2 K), respectively. Surface solar absorptivity and emissivity are also based on TRNSYS defaults: 0.6 and 0.9, respectively. To account for ceiling plenums, they were each roughly approximated as a pair of 90 mm thick horizontal planar airspaces (top and bottom air layers) with a combined thermal resistance of 0.27 (m^2 K)/W (ASHRAE 2009b). The modeling results are likely insensitive to this resistance parameter, because it is a relatively small part of the resistance of each associated assembly.

Zones	Surface	Material (Inside --> Outside)	Thickness mm	Thermal Conductivity W/(m K)	Thermal Capacity kJ/(kg K)	Density kg/m^3	Thermal Resistance (m^2 K)/W Layer	Total
Interior Zones	Roof	Gypsum board	9	0.175	1.134	910	0.05	
		Airspace	N/A	N/A	N/A	N/A	0.27	
		Insulation board	110	0.037	1.26	28	2.96	
		Concrete	210	1.517	0.882	2400	0.14	
		Lightweight concrete	50	1.400	0.93	1800	0.04	
		Asphalt roll	20	0.741	1.51	920	0.03	3.48
	Exterior Wall	Gypsum board	9	0.175	1.134	910	0.05	
		Insulation board	90	0.037	1.26	28	2.42	
		Concrete	200	1.517	0.882	2400	0.13	2.60
	Wall Adjacent to Interior Zones	Gypsum board	9	0.175	1.134	910	0.05	
		Insulation board	65	0.037	1.26	28	1.75	
		Concrete	150	1.517	0.882	2400	0.10	1.90
	Walls Between Apartments & Between Interior Zones	Gypsum board	9	0.175	1.134	910	0.05	
		Concrete	150	1.517	0.882	2400	0.10	
		Gypsum board	9	0.175	1.134	910	0.05	0.20
	Radiant Floor	Wood floor	8	0.112	2.093	900	0.07	
		Mortar (equivalent)	60	2.840	0.882	1000	0.02	
		Active layer	N/A	N/A	N/A	N/A		
		Mortar (equivalent)	20	2.840	0.882	1000	0.01	
		Insulation board	55	0.037	1.26	28	1.48	
		Concrete	210	1.517	0.882	2400	0.14	
		Airspace	N/A	N/A	N/A	N/A	0.27	
		Gypsum board	9	0.175	1.134	910	0.05	2.04
Balconies	Roof	Gypsum board	9	0.175	1.134	910	0.05	
		Airspace	N/A	N/A	N/A	N/A	0.27	
		Insulation board	110	0.037	1.26	28	2.96	
		Concrete	210	1.517	0.882	2400	0.14	
		Lightweight concrete	50	1.400	0.93	1800	0.04	
		Asphalt roll	20	0.741	1.51	920	0.03	3.48
	Exterior Wall	Concrete	150	1.517	0.882	2400	0.10	0.10
	Wall Between Balconies	Gypsum board	9	0.175	1.134	910	0.05	
		Insulation board	65	0.037	1.26	28	1.75	
		Concrete	150	1.517	0.882	2400	0.10	1.90
	Wall Adjacent to Interior Zones	Gypsum board	9	0.175	1.134	910	0.05	
		Insulation board	65	0.037	1.26	28	1.75	
		Concrete	150	1.517	0.882	2400	0.10	1.90
	Floor	Wood floor	8	0.112	2.093	900	0.07	
		Mortar	40	1.422	0.882	2000	0.03	
		Lightweight concrete	40	1.400	0.93	1800	0.03	
		Insulation board	20	0.037	1.26	28	0.54	
		Concrete	210	1.517	0.882	2400	0.14	0.80

Table 3: Opaque element material properties

Figure 7 shows the floor geometry supplied by GREX for the interior zones.

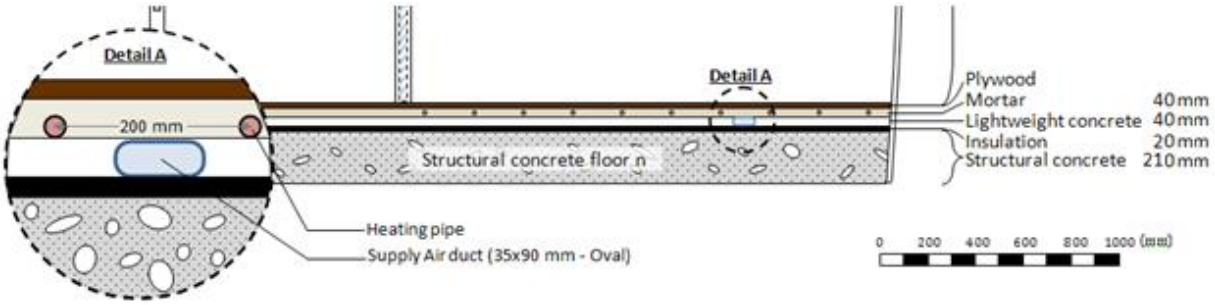

Figure 7: Supplied interior zone floor geometry

To model this floor, using an approach similar to that used by Song et al. (2007) for radiantly-cooled floors, a TRNSYS "active layer" was defined as part of the floor description for interior zones. The layer is called "active" because it contains water-filled pipes that heat the surrounding surfaces when the hydronic system boiler and pump are operating. This is a convenient way to model the floor, but TRNSYS limitations and constraints forced us to use a layout somewhat different from reality, as shown in Figure 8.

In particular, the supply air duct cannot be modeled directly using the "active layer", but can be modeled instead as a separate duct with the exterior surface temperature set to the active layer temperature. Furthermore, to remain within the limits of the active layer model's capabilities (Koschenz et al. 2000), there are several geometry and material property constraints in TRNSYS: (1) the layer thickness immediately above the active layer must be at least 30% of the pipe spacing, (2) the layer thickness below the active layer must be at least half the outside diameter of the pipe, (3) the same material must be used above and below the active layer, and (4) the insulation layer must have a minimum thermal resistance of 0.825 (m^2 K)/W.

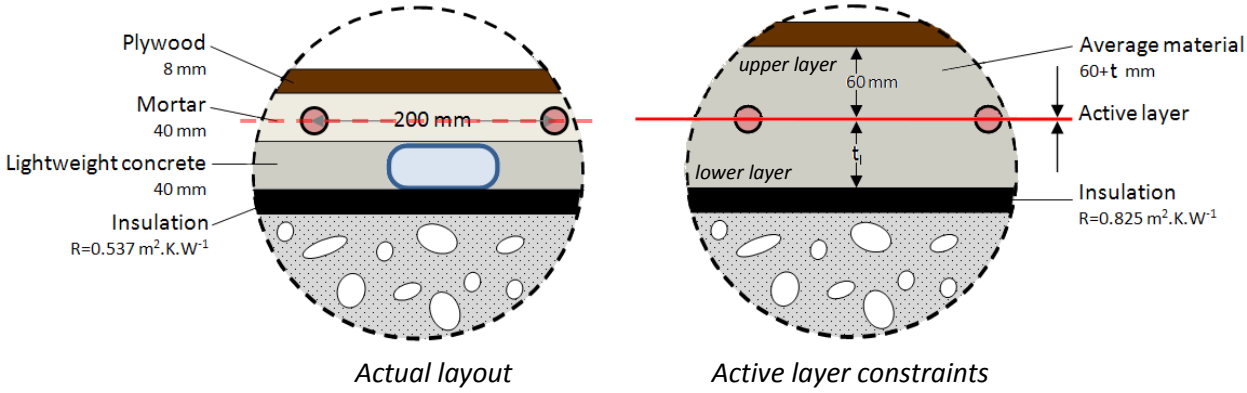

Figure 8: Comparison between the actual floor layout and the active layer constraints

To comply with these constraints, we calculated thermal resistance and thermal capacitance values for an equivalent mortar located above and below the active layer that together matches the combined thermal resistance and thermal capacitance of the actual mortar and lightweight concrete layers. Table 3 lists the resulting properties for the mortar equivalent that surrounds the active layer in the model. For this model, pipe spacing is 200 mm center to center, pipe outside diameter is 20 mm, pipe wall thickness is 2 mm, and pipe wall conductivity is 0.38 W/(m K). The conductivity assumes cross-linked polyethylene (PEX) tubing is used (Watson and Chapman 2002).

Exterior windows for the balcony spaces are single-glazed while interior windows and glazed doors (between balcony spaces and interior spaces) are double-glazed. All glazed elements are horizontal sliders. The single-glazed elements were modeled using TRNSYS glass ID#1001 and the double-glazed elements were modeled using glass ID#1002. Detailed thermal properties for the windows are listed in Table 4.

Windows	Single-glazed	Double-glazed
Thickness, mm	4	4+16+4
Gas fill	N/A	Air
Overall U-value, W/(m^2 K)	5.68	2.83
Solar transmittance ratio	0.830	0.693
Solar reflectance ratio	0.075	0.126
Solar heat gain coefficient	0.855	0.755

Table 4: Glazing properties

Building Air Leakage

The effective leakage area (ELA4) range for 30 Korean apartment buildings based on measured air-tightness data (Lee and Kim 2008) is about 1.5 to 3.2 cm^2/m^2 of floor area; the average is 2.4 cm^2/m^2. If CONTAM had been used, we would simply use this average and normalized leakage data from Lee et al. (2006) for interior windows and doors to disaggregate the total leakage into component leaks. Because we used the LBNL infiltration model instead, another step was needed: recombine the component leaks associated with each zone, and adjust these values as shown in Table 5 to achieve airflow estimates using the LBNL infiltration model that are similar to those estimated using CONTAM with component leaks and closed windows and doors. Consequently, the adjusted values should be considered to be only simple multipliers and not actual leakage areas. In the infiltration model, we used stack and wind coefficients for a one-storey house with no obstructions or local shielding: 0.000145 and 0.000319, respectively. Operable windows and doors were modeled with openable areas as listed in Table 5.

From Zone	To Zone	Adjusted Effective Leakage Area (cm^2)	Openable Area (m^2)
Exterior	Balcony S	879	19.5
Exterior	Balcony N	321	5.4
Balcony S	Zone A	171	4.8
Balcony S	Zone B	66	2.1
Balcony N	Zone A	66	2.1
Balcony N	Zone B	14	2.1
Zone A	Zone B	14	2.1

Table 5: Apartment leakage distribution for use in LBNL infiltration model

Window and door opening schedules are listed in Appendix A. The "summer" season window opening schedule applies from June 1 through August 31 inclusive.

Occupancy and Internal Heat Gains

Data for occupancy and internal heat gains in the two interior zones are based on Yoon et al. (2008). Figure 9 shows the occupancy schedule. The balconies are assumed to be unoccupied. The heat gains from occupants are based on ISO 7730 (2005), as supplied in TRNSYS for apartments (120 W/person, 60% sensible, 40% latent).

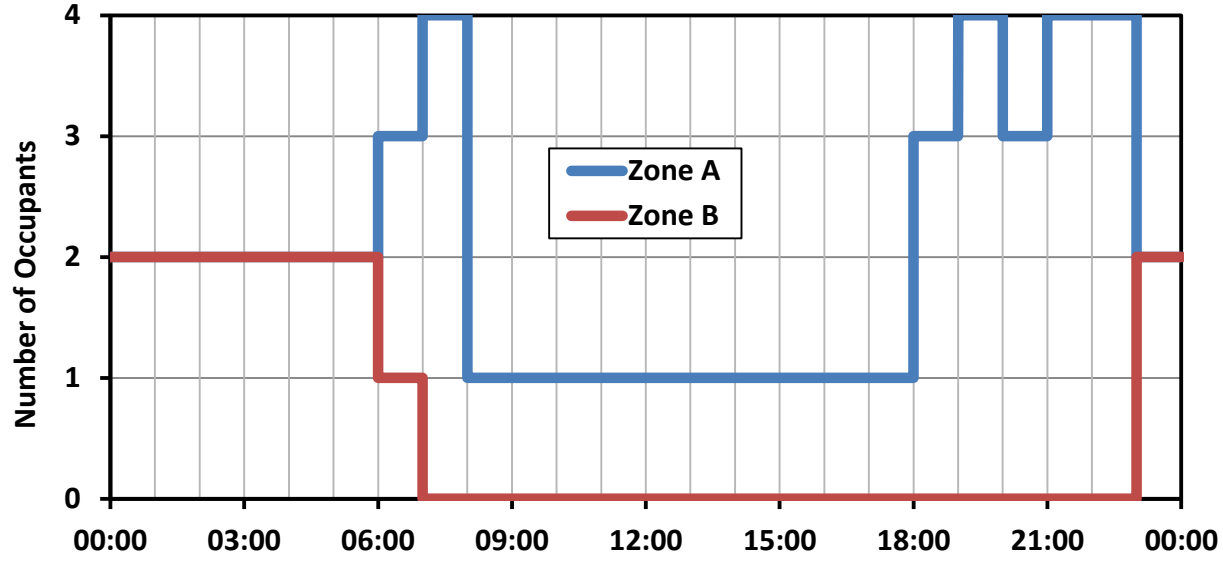

Figure 9: Interior zone occupancy schedule

Lighting loads in interior zones A and B are a maximum of 422 W and 126 W, respectively (60% radiative and 40% convective). Equipment loads in zone A are a maximum of 936 W (26% radiative and 74% convective). There are no lighting loads for the balconies, and no equipment loads except in zone A. Figure 10 and Figure 11 show the lighting and equipment load schedules, respectively.

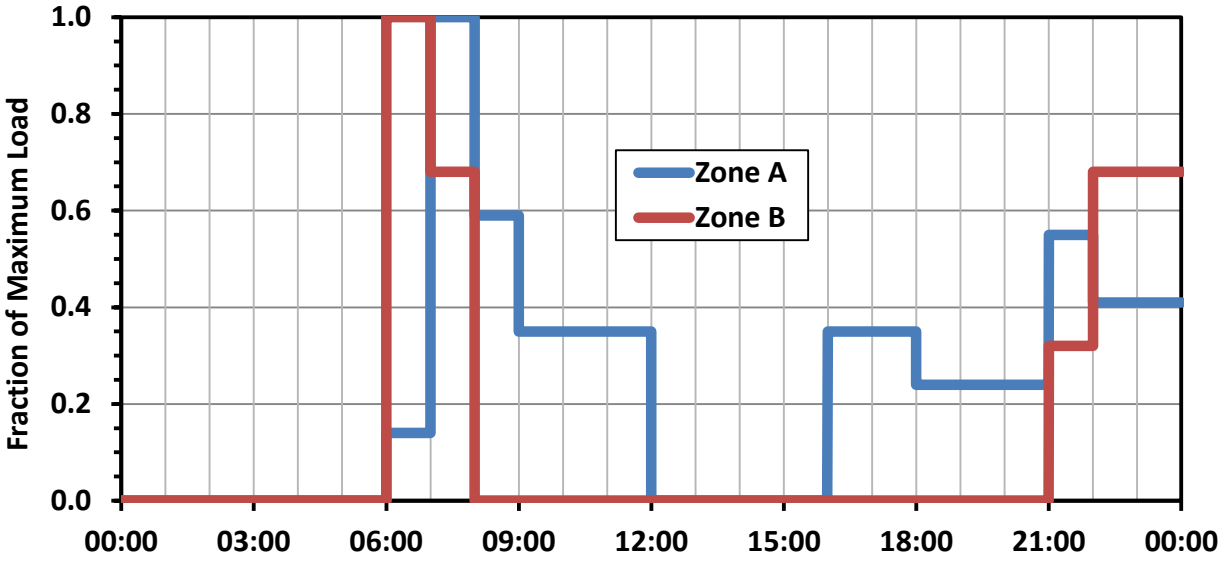

Figure 10: Lighting schedule – Interior zones A and B

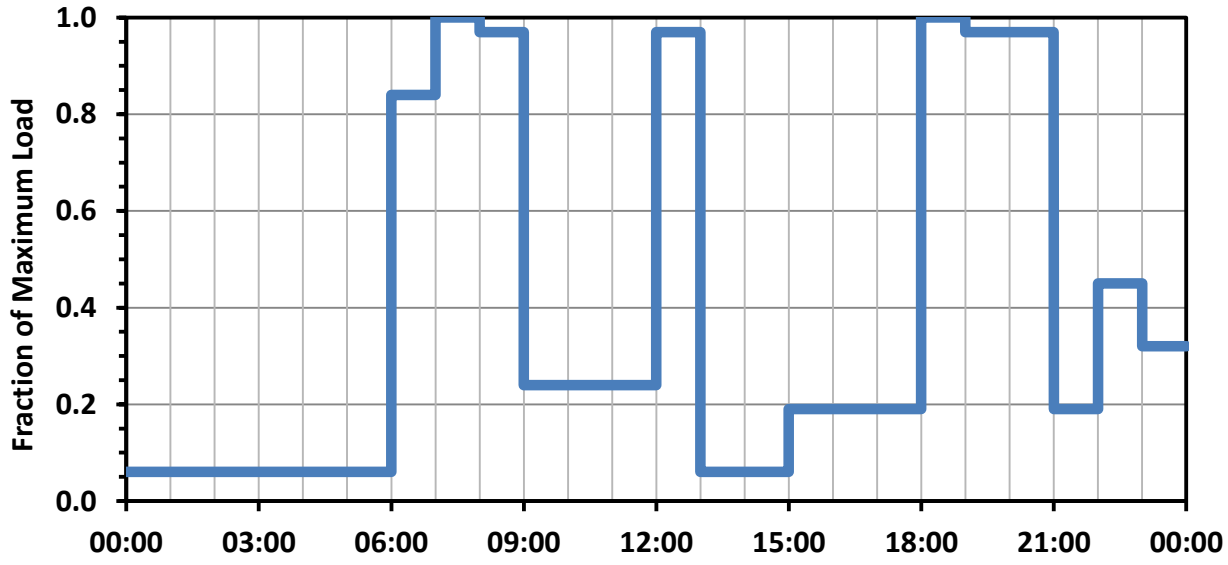

Figure 11: Equipment schedule – Interior zone A

Mechanical Ventilation Systems

To reiterate, two balanced ventilation systems were modeled: an HRV system and the non-HRV GREX system. Both systems continuously supply air to and exhaust air from the interior zones to achieve the required 0.7 ACH ventilation target. As a result, based on the zone volumes, 135 m^3/h and 60.5 m^3/h are supplied to and exhausted from zones A and B, respectively. The total flow is 195.5 m^3/h (about 54 L/s). The kitchen range hood in zone A was not modeled in either case because it rarely operates.

The HRV system consists of a heat exchanger, two fans, an electric preheater, and supply and exhaust ducts. The heat exchanger sensible effectiveness is 0.77, which, as Figure 12 shows, is roughly the most common value for HRVs with supply flows near 54 L/s at 0°C (HVI 2011).

The HRV supply and exhaust fans are located in the associated airflow paths downstream of the heat exchanger. Based on rated HRV flow (150 m^3/h), static pressure rise (117.5 Pa), and power (45 W) data supplied by GREX for the HRV, the corresponding combined fan and motor efficiency is 11%. Assuming that this efficiency is constant and using static pressure rise versus flow data from Chang and Hong (2008) for a fan driven by a constant speed motor, we calculated that the static pressure rise and power of each fan for a 195.5 m^3/h flow is approximately 105 Pa and 53 W, respectively. Therefore, the total power for the HRV supply and exhaust fans combined is 106 W.

The HRV preheater is located *upstream* of the heat exchanger in the supply airstream. Its power input to the supply air is 1.2 kW whenever the inlet supply air (outdoor air) temperature is less than 5°C.

Supply and exhaust ducts for the HRV are located in the ceiling plenums. The outer surface of each duct is assumed to be at the same temperature as the ceiling plenum air through which it passes (we assume that the plenums and conditioned spaces below are at approximately the same temperature). The supply duct serving zone A passes through zone B first and then into zone A. It is 50 mm in diameter and is 5.1 m long in each zone. The convective heat loss coefficient for this duct is 38 W/(m^2 K), based on forced convection correlations for turbulent flow through tubes (Incropera and DeWitt 1981). The supply duct serving zone B is the same, but is 7 m in length and, with less airflow, has a lower convective heat loss coefficient: 23 W/(m^2 K).

Because exhaust air temperatures are approximately the same as zone air temperatures, heat transfer between the zone air and the exhaust ducts is not modeled.

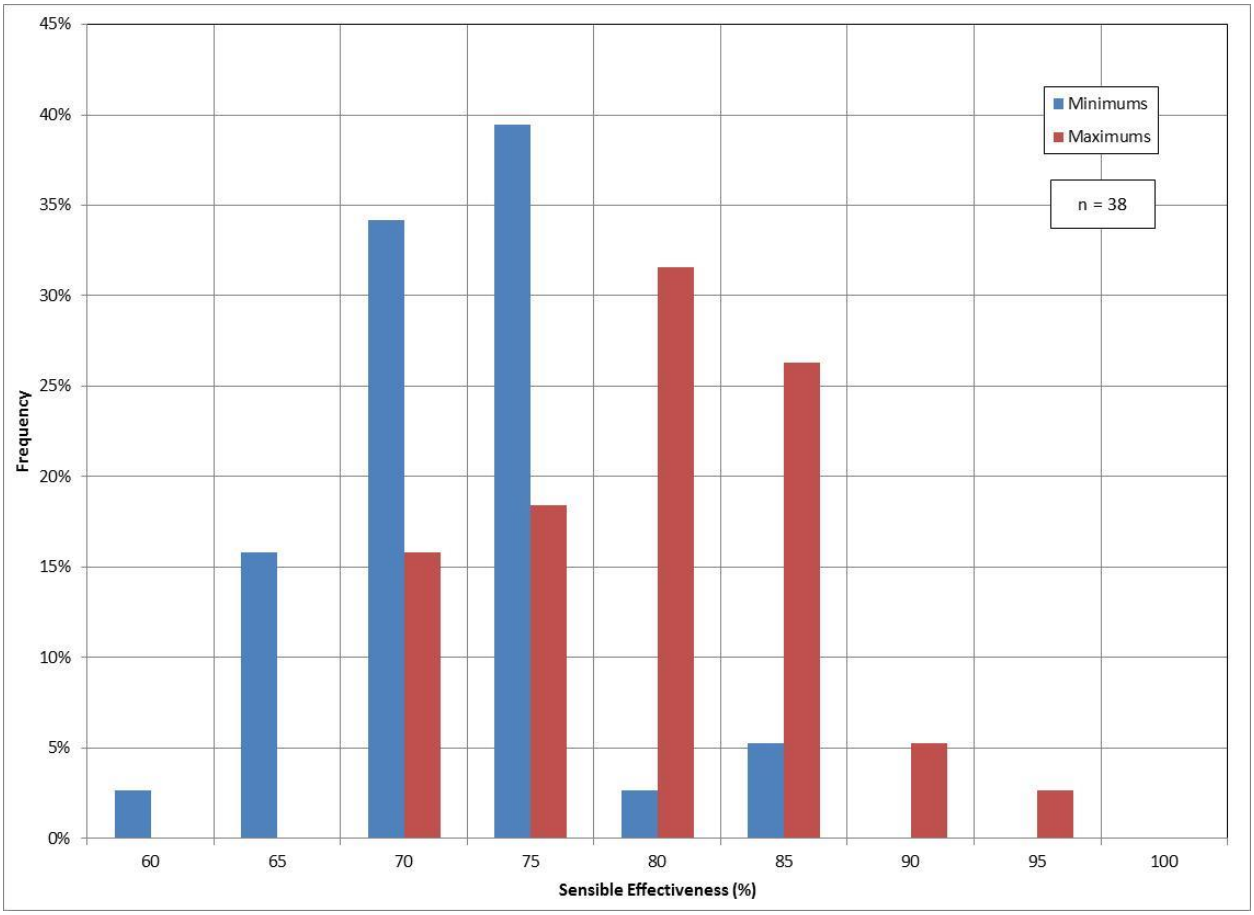

Figure 12: HRV sensible effectiveness data from HVI (2011)

The GREX system uses a fan to supply ventilation air through ducts embedded in lightweight concrete between floor radiant heating panels and an insulation layer beneath the panels. Heat transfer from the floor preheats the supply air before it enters the conditioned spaces. In the version of the system that we simulated, to prevent excessive pressurization of the conditioned spaces, an exhaust system consisting of bathroom exhaust fans and ducts located in ceiling plenums is used.

The GREX supply fan is located near the inlet of the supply duct. Based on static pressure rise and power versus flow data provided by GREX for the specified DSE-400 supply fan, we calculated that the static pressure rise and power for a 54 L/s flow is approximately 169 Pa and 75 W, respectively.

Data provided by GREX indicate that each of the two bathroom exhaust fans has a rated flow and power of 90 m^3/h (25 L/s) and 37 W, respectively. Pressure rise and power versus flow data were not provided, however, so we cannot calculate the fan and motor efficiency or the pressure rise and power at the flow used in the simulations. Therefore, in the absence of these data, we have assumed that the total power for the two exhaust fans combined is the same as the power for the supply fan: 75 W (which is also roughly double the rated power of one exhaust fan).

The supply ducts in the GREX system are located in the floor assembly and in the walls. For the ducts in the floor, the duct outer surface is assumed to be at the same temperature as the

active layer through which it passes. For the ducts in the wall, the duct outer surface is assumed to be at the same temperature as the wall surface facing the zone being served. Like the HRV system, the supply duct serving zone A passes through zone B first and then into zone A. The floor section has a flat oval shape (35 mm high by 90 mm wide) and is 5.1 m long in each zone. The convective heat loss coefficient for this duct is 37 W/(m^2 K). The wall duct section is 50 mm in diameter and 2.3 m long. The convective heat loss coefficient for this duct is 38 W/(m^2 K). The supply duct serving zone B is the same, but is 7 m in length through the floor and 2.3 m long in the wall. The convective heat loss coefficients for these duct sections are 22 and 23 W/(m^2 K), respectively.

Like the HRV system, because exhaust air temperatures are approximately the same as zone air temperatures, heat transfer between the zone air and the exhaust ducts is not modeled.

Hydronic Heating System

A low-temperature hydronic system supplies hot water to floor heating panels and operates from September 15 through May 15 inclusive. It consists of a natural-gas-fired boiler, a circulating pump, manifolds, pipes, control valves, and zone thermostats. The hydronic system does not have separate primary and secondary circuits nor does it use mixing valves so that the primary circuit (boiler water) can temper the water circulated in the secondary circuits. Instead, flow through each parallel floor heating loop is controlled by a two-way valve that is either open or closed as needed to maintain the associated zone air temperature set point (23 ± 0.56°C), as sensed by the room air thermostat in that zone. Both zone air thermostats are connected together to a valve controller, which determines the total system flow rate needed and the fraction of total system flow that passes through each valve.

The boiler is a Kiturami "Eco Condensing Gas Boiler". A preliminary simulation of the GREX system with design weather conditions and a 100kW boiler was used to determine the maximum required boiler output capacity, assuming the boiler supplies 55°C water to the floor and cycles on and off to maintain the interior zone air temperatures. Design conditions were: -11°C outdoor air temperature, 50% relative humidity, no wind, no solar radiation, no occupants, no internal gains, and closed doors and windows. The resulting output capacity is 20.6 kW. Based on data provided by GREX, the closest size for a Kiturami boiler is 23.3 kW, which we used in subsequent simulations with actual weather. In our simulations, total zone heating loads exceeded boiler capacity only about 0.5% of the time due to actual outdoor air temperatures being below the design temperature (minimum outdoor air temperature is -14.9°C). When boiler capacity was exceeded, slightly cooler water was supplied by the boiler to the floors. The boiler efficiency (output power divided by input power) is 88% based on the provided Kiturami data.

The constant speed circulating pump is a Kiturami model KP-081-G and is located downstream of the boiler. Based on data provided by GREX for this pump, and on the peak water flow required to meet interior zone loads (1400 kg/h, or about 23 L/s, with 69% to zone A and 31% to zone B), the pump power is 98 W. Like the boiler, the pump cycles on and off in response to thermostat calls for heating.

Heat exchange between the building and the hydronic system pipes and manifolds that connect the boiler, pump, and floor loops together is likely small compared to other processes and was not modeled.

TRNSYS Component Assembly Panel

In TRNSYS, model components are linked together using a graphical user interface called the assembly panel. Figure 13 shows an overview of the assembly panel. Links are shown as lines between components with arrows that show nominal data flow directions.

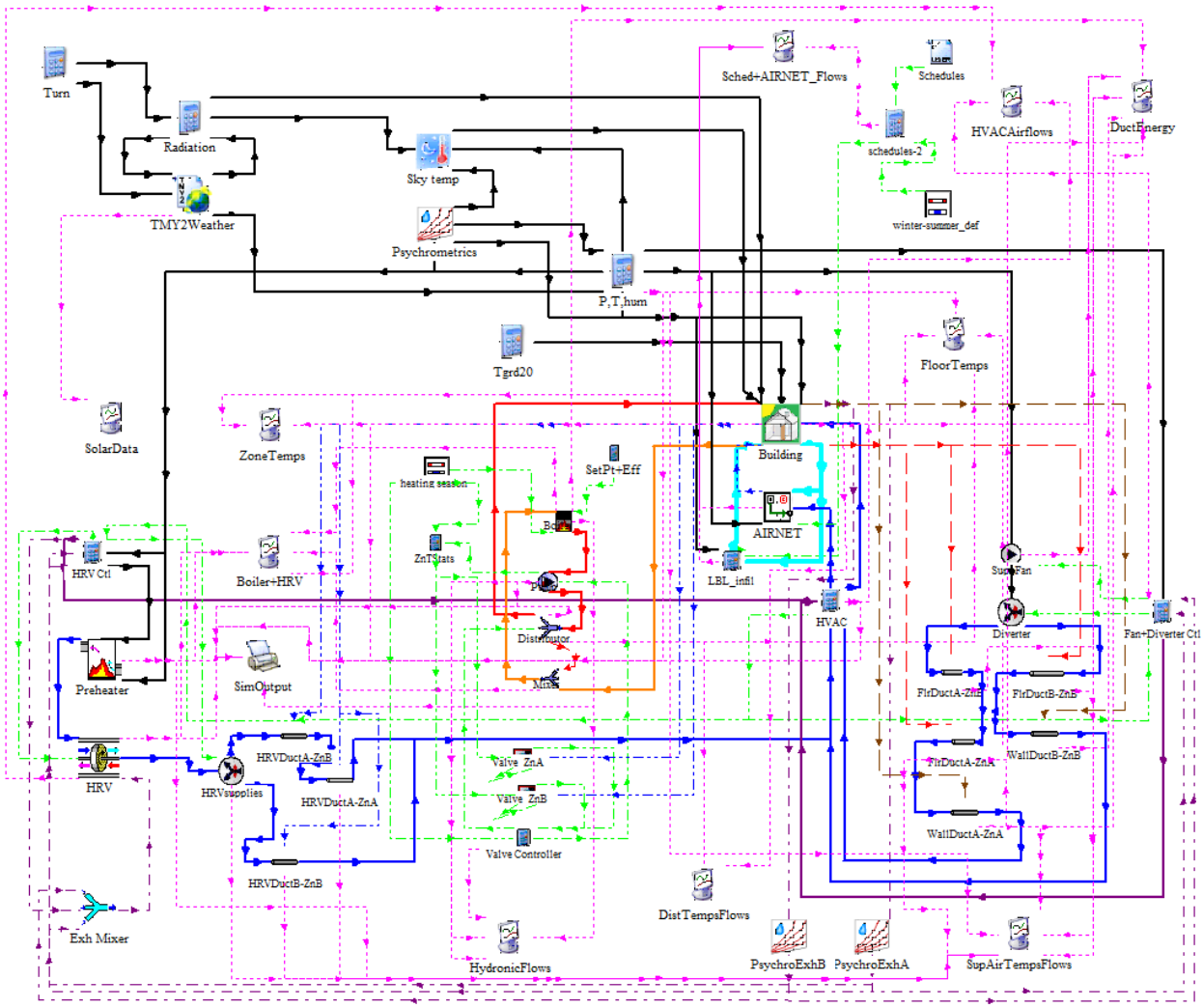

Figure 13: TRNSYS module assembly panel

The information shown in Figure 13 can be grouped into seven parts:

1. Building thermal module (Type56), unused "AIRNET" airflow network analysis module (Type 97), which also reads a CONTAM input file, and the LBNL infiltration calculator, along with their links (approximately middle of the figure),
2. Hydronic system components and links (to the left of the building model),
3. HRV system components and links (lower left),
4. GREX system components and links (lower right),
5. Weather data reading and processing components and links (top left),
6. Schedule reading components and links (top right), and
7. Output components (distributed throughout with magenta links).

SIMULATION RESULTS

As an example to illustrate system dynamics, Figure 14 displays the outdoor air temperature (light blue) and several GREX system temperatures for interior zone A during the first week of January: the hot water entering the floor (gold), the floor active layer node (midway between heating pipes, red), the floor upper surface (brown), the supply air (light orange), and the room air (dark blue). The room air temperature for zone B is also shown (dark pink).

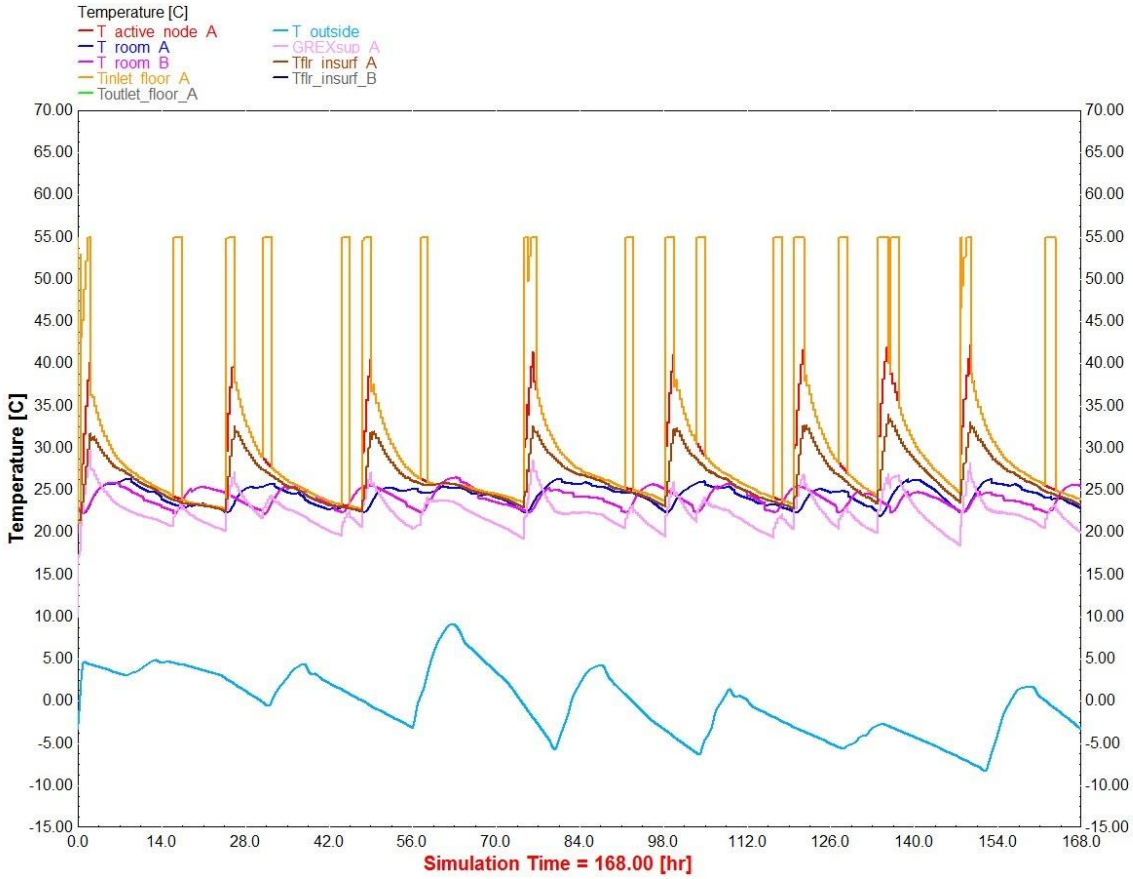

Figure 14: Sample plot of GREX system temperatures

When room air temperatures exceed their control range (23±0.56°C), the hydronic system cycles on and off to provide hot water to the floors in zones A and/or B. Cycling rates and the length of "on" periods increase as the outdoor air temperature decreases. The supply air temperature for zone A is affected by zone A and B floor heating, because the duct passes through the floors of both zones. Supply air temperatures range from about 18°C to 28°C, and their variability is strongly coupled to the supply of hot water from the boiler.

The active node temperatures in zone A, which are also the supply duct exterior surface temperatures in that zone, range from about 23°C to 43°C. The floor surface temperatures in zone A fluctuate between about 23°C and 34°C, which approximates the experimental results of Hwang et al. (2008) for a raised-floor with hot-water radiant heating and underfloor ventilation.

The room air temperature for zone A fluctuates between about 22°C and 26°C. Temperatures outside the thermostat set point range are due to the time lag between sensing air temperatures and subsequent warming or cooling of the radiant floor mass. The higher air temperatures are also due to "uncontrolled" heat gains from occupants, lighting, equipment, and solar radiation.

Except for the supply air temperatures, as discussed later, results for the HRV system are similar. Figure 15 shows a sample plot for the HRV system, which includes air temperatures at its preheater exit.

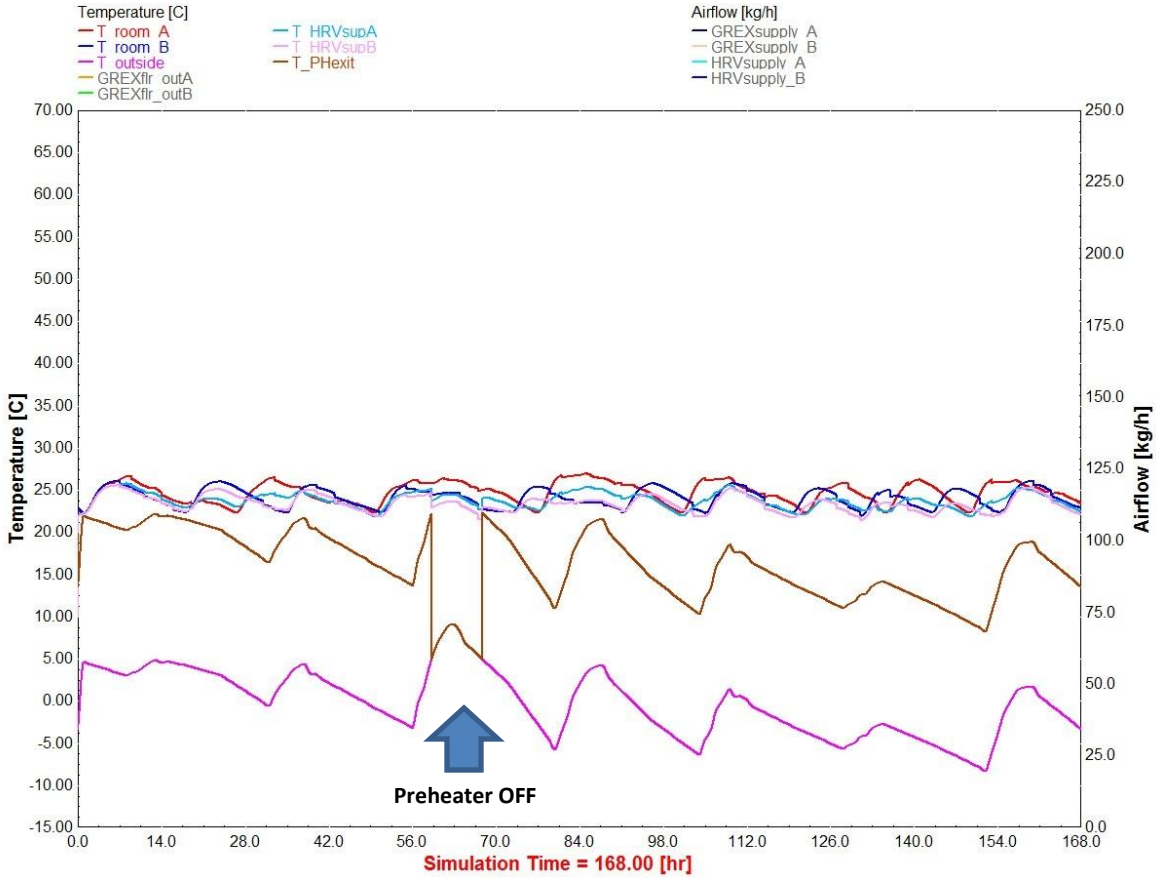

Figure 15: Sample plot of HRV system temperatures

The HRV preheater cycles on whenever the outdoor air temperature is less than 5°C, and results in air temperatures entering the HRV heat exchanger that sometimes are near the HRV exhaust air inlet temperature (flow-weighted combination of room air temperatures). Small differences between the heat exchanger supply air and exhaust air inlet temperatures reduce the amount of heat that can be recovered. In Figure 15, the preheater is off only for a brief period.

Appendix B compares the results from our annual simulations of the HRV and GREX ventilation systems during the heating season. Minimum, maximum, and average values in those tables are not necessarily coincident. In summary:

1. Room air temperatures are almost identical for the two systems, and so are floor surface temperatures. In general, differences (even for minimums and maximums) are less than 1°C.
2. On average, the GREX supply air temperatures are about 1°C cooler. Figure 16 shows the distribution of *coincident* supply air temperature differences between the two systems. In each zone, the GREX system supplies air within ±4°C of the HRV system supply air temperature (cooler or warmer) 95% of the time and within ±2°C 70% of the time. Although not shown in Appendix B or Figure 16, our analyses indicate that 99% of the GREX supply air temperatures for zones A and B are warmer than 19.3°C and 18.7°C, respectively. For the HRV system, 99% of these temperatures are warmer than 21.6°C and 21.3°C, respectively.

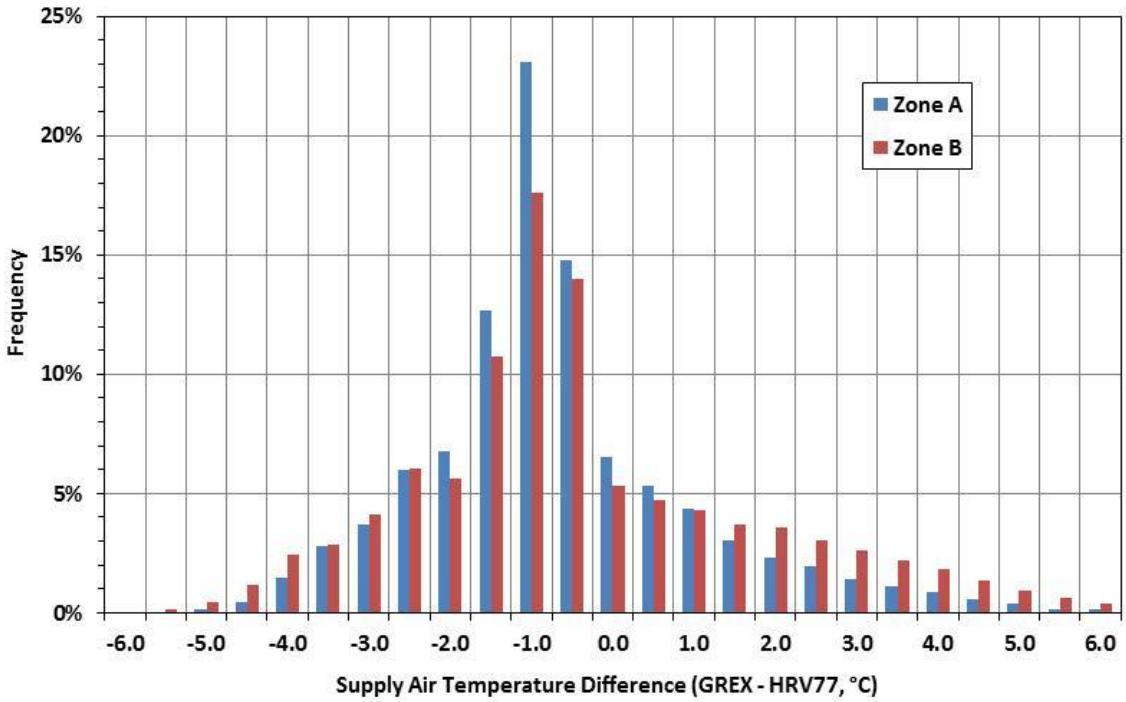

Figure 16: Comparison of coincident differences between system supply air temperatures

3. Although the GREX system uses about 3% more boiler energy, 1% more pump energy, and 42% more fan energy annually relative to the HRV system, its total annual energy use is only about 78% of the total annual energy use of the HRV system. The difference in annual totals is largely because the GREX system does not have an electric preheater. Preheater energy is about 27% of the HRV system total annual energy. Because the preheater is configured to operate at full power (1.2 kW) whenever the outdoor temperature is below 5°C, and the outdoor temperature is below this value about 47% of the time during the heating season, the preheater also operates during about 47% of the heating hours.

As Figure 12 shows, HRV sensible effectiveness has a wide range. To examine the sensitivity of our results to this parameter, we simulated the same HRV system but with a low effectiveness: 60%. Appendix C compares the results of our annual simulations for the two HRV cases during the heating season. Again, minimum, maximum, and average values in those tables are not necessarily coincident. In summary:

1. Reducing the HRV effectiveness from 77% to 60% has almost no impact on room air temperatures, floor surface temperatures, and annual energy use. In general, the temperature differences between the two cases (even for minimums and maximums) are 0.2°C or less. The total annual energy use increased by only 2% when the effectiveness was reduced. The insensitivity is largely due to the operation of the preheater, which reduces the temperature difference between the heat exchanger inlet streams and hence the amount of heat that can be recovered.
2. On average, the supply air temperatures with the lower effectiveness are about 1°C cooler (somewhat closer to the GREX system values).

REFERENCES

ASHRAE. 2009a. Handbook of Fundamentals – Ventilation and Infiltration. Atlanta: American Society of Heating, Refrigerating, and Air-Conditioning Engineers, Inc. pp. 16.23-16.25.

ASHRAE. 2009a. Handbook of Fundamentals – Heat, Air, and Moisture Control in Building Assemblies – Material Properties. Atlanta: American Society of Heating, Refrigerating, and Air-Conditioning Engineers, Inc. p. 26.3.

CEC. 2008. Residential Alternative Calculation Manual (ACM) Approval Method. 2008 Building Energy Efficiency Standards. California Energy Commission CEC-400-2008-002-CMF. December. p. 3-10.

Chang, H-J. and S-J. Hong. 2008. A Study on the Performance of Heat Recovery Ventilators for Apartment Houses. School of Architectural Engineering, Hongik University, Yeongi-gun, Korea and Architectural Technology Research Team, DAEWOO E&C, Suwon, Korea.

HVI. 2011. HVI Tested/Certified Heat Recovery Ventilators and Energy Recovery Ventilators. February 1.

Hwang, W-J., Y-M. Kim, and J-Y. Sohn. 2008. A Study on Thermal Environment of the Raised-Floor Ondol with a Ventilation System at an Apartment. Hanyang University, Seoul.

Incropera, F.P. and D.P. DeWitt. 1981. Fundamentals of Heat Transfer. New York: John Wiley and Sons. pp. 406-412.

ISO. 2005. ISO 7730:2005 - Ergonomics of the Thermal Environment - Analytical Determination and Interpretation of Thermal Comfort using Calculation of the PMV and PPD Indices and Local Thermal Comfort Criteria. Geneva: International Organization for Standardization.

Kim, J-S., S-A. Moon, T-G. Lee, S-J. Moon, and J-H. Lee. 2009. Calculation of Heating Load for an Apartment Complex with Unit Building Method. International Journal of Engineering and Applied Sciences 5:3.

Koschenz, M., B. Lehmann, and S. Holst. 2000. Thermoaktive Bauteilsysteme TABS – Eine Einfache und Trotzdem Genaue Methode zur Modellierung. Beitrag am TRNSYS-Usertag, 25 Februar, Stuttgart-Weillmdorf.

Lee, Y-G. and S-S. Kim. 2008. Technical Note AIVC 64: Ventilation in Korea. Air Infilitration and Ventilation Centre (AIVC). Sint-Stevens-Woluwe, Belgium.

Lee, Y-G., T. Kim, and J. Yoon. 2006. Development of a Ventilation Performance Prediction Equation for Korean Multi-Family Housing Using Airflow Analysis. November, Journal of Asian Architecture and Building Engineering, Vol. 5.2, p. 371.

McDowell, T.P. et al. 2003. Integration of Airflow and Energy Simulation Using CONTAM and TRNSYS. ASHRAE Transactions - Symposium KC-03-10.

Song, D. et al. 2007. Performance Evaluation of a Radiant Floor Cooling System Integrated with Dehumidified Ventilation. Applied Thermal Engineering, Vol. 28, pp. 1299-1311.

Watson, R.D. and K.S. Chapman. 2002. Radiant Heating and Cooling Handbook. New York: McGraw-Hill. pp. 5-74:5-75

Yeo, M-S., I-H. Yang, and K-W. Kim. 2003. Historical Changes and Recent Energy Saving Potential of Residential Heating in Korea. Energy and Buildings, Vol. 35, pp. 715-725.

Yoon, S-H. et al. 2008. Energy Saving Effects according to the Window Performance for an Apartment House and the Estimation of the Window Economical Efficiency. pp. 321-330.

APPENDIX A. WINDOW AND DOOR OPENING SCHEDULES

WINDOWS

Balcony N and S Exterior Windows (Fall-Winter-Spring)

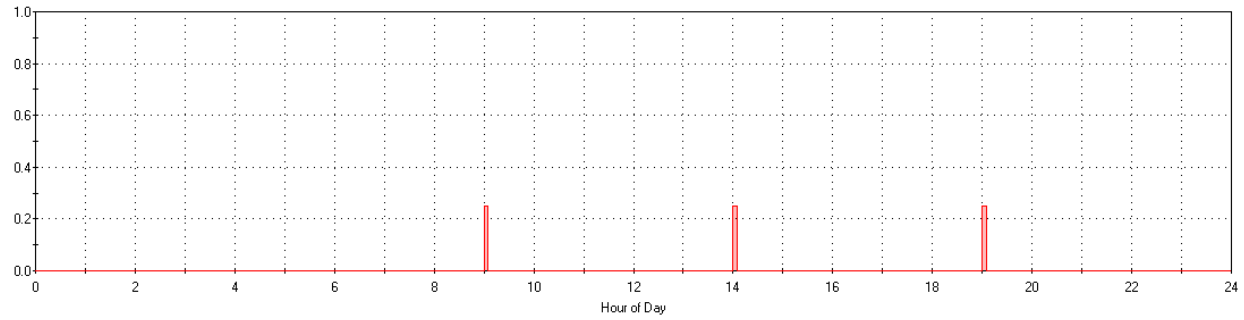

Balcony N and S Exterior Windows (Summer)

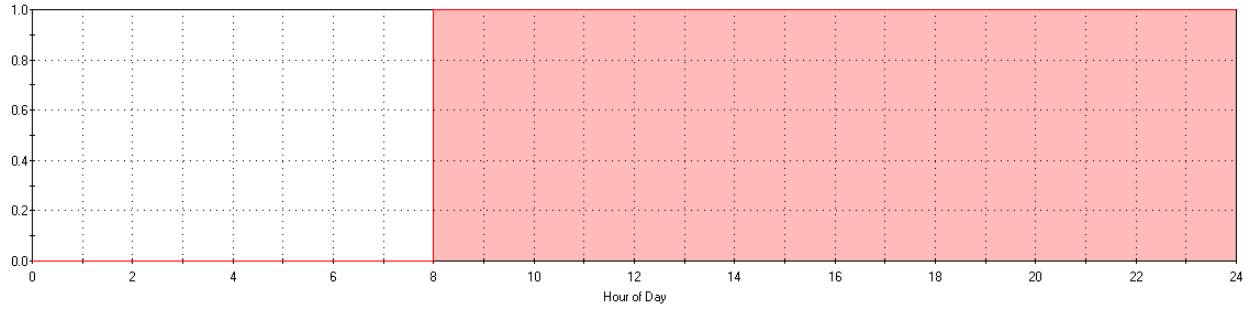

Interior Windows (Fall-Winter-Spring)

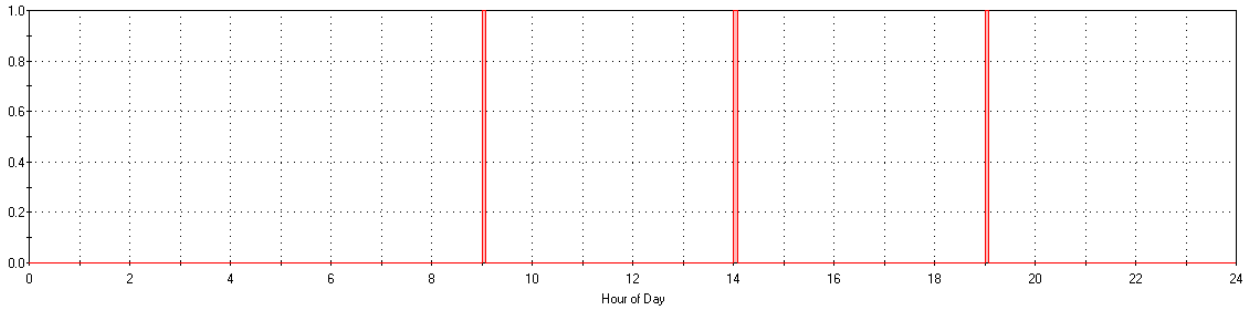

Interior Windows (Summer)

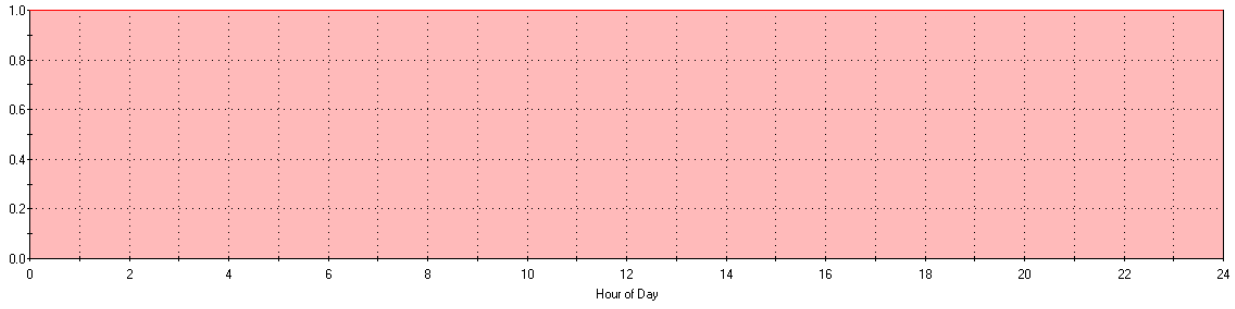

Figure 17: Window opening schedules

DOORS

Door between Zones A and B

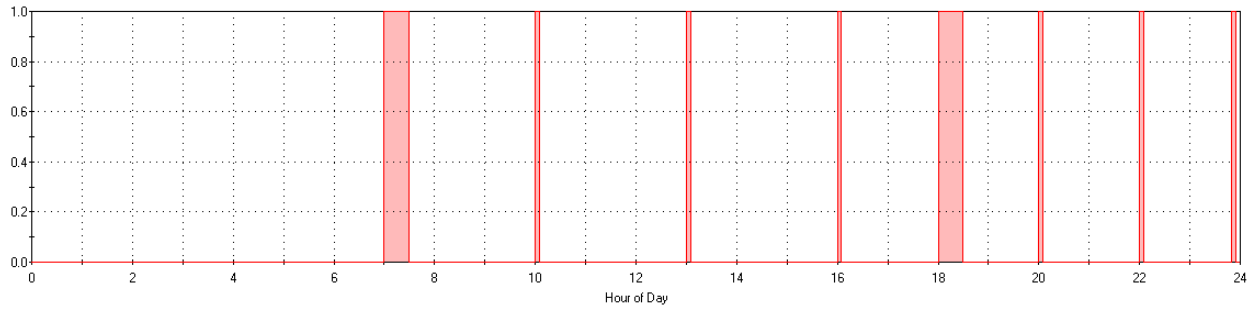

Door between Balcony N and Zone B

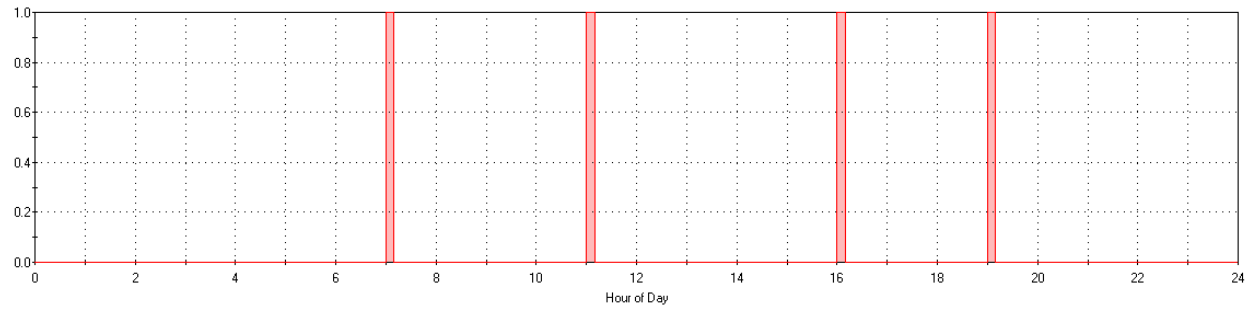

Figure 18: Door opening schedules

APPENDIX B. HRV AND GREX SYSTEM COMPARISONS

Simulation Results Summary: Heating Season (Sep 15 through May 15)

Table B1: Heating and Ventilating Equipment Site Energy Use (kWh)

System Component	HRV77 System	GREX System	GREX/HRV77 Fraction
Boiler Input	8,395	8,634	1.03
Hydronic Pump	60	61	1.01
Supply and Exhaust Fans	618	875	1.42
HRV Preheater	3,283	N/A	N/A
Total	**12,263**	**9,570**	**0.78**

Table B2: Room Air Temperatures (°C); Setpoint: 23.0 ± 0.56°C

	HRV77 System		GREX System		GREX-HRV77 Difference	
Statistic	**Zone A**	**Zone B**	**Zone A**	**Zone B**	**Zone A**	**Zone B**
Minimum	21.9	21.0	21.6	20.7	-0.3	-0.3
Maximum	34.2	31.7	33.7	31.3	-0.5	-0.4
Average	25.4	24.6	25.2	24.5	-0.2	-0.1
RMS	2.2	1.6	2.0	1.5	-0.2	-0.1

Table B3: Room Air Underheating and Overheating Time Fractions (%)

	HRV77 System		GREX System		GREX-HRV77 Difference	
Statistic	**Zone A**	**Zone B**	**Zone A**	**Zone B**	**Zone A**	**Zone B**
Below 22.44°C	1.0	1.5	0.8	1.4	-0.2	-0.1
Above 23.56°C	79.9	69.8	78.0	70.2	-1.9	0.4

Table B4: Temperatures of Supply Air Entering Rooms (°C)

	HRV77 System		GREX System		GREX-HRV77 Difference	
Statistic	**Zone A**	**Zone B**	**Zone A**	**Zone B**	**Zone A**	**Zone B**
Minimum	20.8	19.9	17.9	16.9	-2.9	-3.0
Maximum	32.5	31.2	31.3	30.5	-1.2	-0.7
Average	24.3	23.8	23.3	23.2	-1.0	-0.6
RMS	1.9	1.7	2.2	2.3	0.3	0.6

Table B5: Temperatures of Floor Upper Surfaces (°C)

	HRV77 System		GREX System		GREX-HRV77 Difference	
Statistic	**Zone A**	**Zone B**	**Zone A**	**Zone B**	**Zone A**	**Zone B**
Minimum	22.5	22.6	22.5	22.6	0.0	0.0
Maximum	34.9	35.5	35.0	35.0	0.1	-0.5
Average	26.6	26.6	26.5	26.5	-0.1	-0.1
RMS	2.6	2.6	2.5	2.6	-0.1	0.0

APPENDIX C. HRV SYSTEM COMPARISONS

Simulation Results Summary: Heating Season (Sep 15 through May 15)

Table C1: Heating and Ventilating Equipment Site Energy Use (kWh)

System Component	HRV77 System	HRV60 System	HRV60/HRV77 Fraction
Boiler Input	8,395	8,614	1.03
Hydronic Pump	60	63	1.04
Supply and Exhaust Fans	618	618	1.00
HRV Preheater	3,283	3,283	1.00
Total	**12,263**	**12,485**	**1.02**

Table C2: Room Air Temperatures (°C); Setpoint: 23.0 ± 0.56°C

	HRV77 System		HRV60 System		HRV60-HRV77 Difference	
Statistic	Zone A	Zone B	Zone A	Zone B	Zone A	Zone B
Minimum	21.9	21.0	22.0	21.2	0.1	0.2
Maximum	34.2	31.7	33.9	31.5	-0.3	-0.2
Average	25.4	24.6	25.3	24.6	-0.1	0.0
RMS	2.2	1.6	2.1	1.5	-0.1	-0.1

Table C3: Room Air Underheating and Overheating Time Fractions (%)

	HRV77 System		HRV60 System		HRV60-HRV77 Difference	
Statistic	Zone A	Zone B	Zone A	Zone B	Zone A	Zone B
Below 22.44°C	1.0	1.5	1.1	1.6	0.1	0.1
Above 23.56°C	79.9	69.8	78.8	70.7	-1.1	0.9

Table C4: Temperatures of Supply Air Entering Rooms (°C)

	HRV77 System		HRV60 System		HRV60-HRV77 Difference	
Statistic	Zone A	Zone B	Zone A	Zone B	Zone A	Zone B
Minimum	20.8	19.9	19.8	19.0	-1.0	-0.9
Maximum	32.5	31.2	31.7	30.5	-0.8	-0.7
Average	24.3	23.8	23.7	23.3	-0.6	-0.5
RMS	1.9	1.7	1.9	1.7	0.0	0.0

Table C5: Temperatures of Floor Upper Surfaces (°C)

	HRV77 System		HRV60 System		HRV60-HRV77 Difference	
Statistic	Zone A	Zone B	Zone A	Zone B	Zone A	Zone B
Minimum	22.5	22.6	22.5	22.5	0.0	-0.1
Maximum	34.9	35.5	34.6	35.4	-0.3	-0.1
Average	26.6	26.6	26.6	26.6	0.0	0.0
RMS	2.6	2.6	2.6	2.7	0.0	0.1